



TITLE:

Usefulness of operative planning based on 3-dimensional CT cholangiography for biliary malignancies.

AUTHOR(S):

Okuda, Yukihiro; Taura, Kojiro; Seo, Satoru; Yasuchika, Kentaro; Nitta, Takashi; Ogawa, Kohei; Hatano, Etsuro; Uemoto, Shinji

CITATION:

Okuda, Yukihiro ...[et al]. Usefulness of operative planning based on 3-dimensional CT cholangiography for biliary malignancies.. Surgery 2015, 158(5): 1261-1271

ISSUE DATE:

2015-11

URL:

<http://hdl.handle.net/2433/203042>

RIGHT:

© 2015. This manuscript version is made available under the CC-BY-NC-ND 4.0 license <http://creativecommons.org/licenses/by-nc-nd/4.0/>; The full-text file will be made open to the public on 1 November 2016 in accordance with publisher's 'Terms and Conditions for Self-Archiving'; This is not the published version. Please cite only the published version.; この論文は出版社版ではありません。引用の際には出版社版をご確認ください。

- 1 1 Title: Usefulness of three-dimensional computed tomography cholangiography for biliary
- 2
- 3
- 4 2 malignancies
- 5
- 6
- 7
- 8 3
- 9
- 10
- 11 4 Authors: Yukihiro Okuda, MD, Kojiro Taura, PhD, Satoru Seo PhD, Kentaro Yasuchika PhD,
- 12
- 13
- 14
- 15 5 Takashi Nitta PhD, Kohei Ogawa PhD, Etsuro Hatano, PhD, Shinji Uemoto, PhD
- 16
- 17
- 18 6
- 19
- 20
- 21
- 22 7 Department of Surgery, Graduate School of Medicine, Kyoto University
- 23
- 24
- 25 8
- 26
- 27
- 28
- 29 9 Disclaimers: None
- 30
- 31
- 32
- 33 10
- 34
- 35
- 36 11 Correspondence and reprint requests to: Kojiro Taura,
- 37
- 38
- 39
- 40 12 54Kawahara-cho, Shogoin, Sakyo-ku, Kyoto 606-8507, Japan
- 41
- 42
- 43 13 Telephone: +81-75-751-4323
- 44
- 45
- 46 14 FAX: +81-75-751-4390
- 47
- 48
- 49
- 50 15 Email: ktaura@kuhp.kyoto-u.ac.jp
- 51
- 52
- 53
- 54 16
- 55
- 56
- 57 17 Source of financial support: None
- 58
- 59
- 60 18
- 61
- 62
- 63
- 64
- 65

Abstract

Background : The complexity of hepatic hilar anatomy is an obstacle to precise diagnosis of tumor spread and appropriate operative planning for biliary malignancies. Three-dimensional (3D) cholangiography and angiography may overcome this obstacle and facilitate curative resection. The objective of this study is to evaluate the impact of 3D computed tomography (CT) cholangiography on operative planning and outcomes of biliary malignancies.

Methods: From 2009 to 2014, 3DCT cholangiography was performed on 49 patients with biliary malignancies requiring major hepatic resection and extrahepatic bile duct resection.

The 3D cholangiogram was merged with 3D angiography and portography to create an all-in-one 3D image of the hepatic hilum. The cutting line of the bile duct and the type of liver resection were determined based on the spatial relationship between tumor spread and the landmark vessels. The necessity of vascular reconstruction was also evaluated. Preoperative imaging and operative findings were compared. Operative curability was compared with that of the historical cohort before the introduction of 3D cholangiography.

Results: Histological examination of the bile duct stump showed a negative margin in 39 (80%), carcinoma in situ in 7 (14%), and invasive cancer in 3 patients (6%) on the first cutting. The invasive cancer-free rate (94%) on the first cutting was superior to that in the

1 1 historical cohort (80%) ($p=0.02$). The necessity for portal/arterial reconstruction was
2
3
4
5 2 predicted with 98%/94% accuracy.
6
7
8 3 Conclusion: 3D cholangiography provides accurate information about hilar anatomy and
9
10
11 4 plays a role in facilitating adequate operative planning.
12
13
14 5
15
16
17
18
19
20
21
22
23
24
25
26
27
28
29
30
31
32
33
34
35
36
37
38
39
40
41
42
43
44
45
46
47
48
49
50
51
52
53
54
55
56
57
58
59
60
61
62
63
64
65

- 1 1 Abbreviations and Acronyms
- 2
- 3
- 4 2 ERC; endoscopic retrograde cholangiography
- 5
- 6
- 7
- 8 3 2D/3D; two-dimensional/ three-dimensional
- 9
- 10
- 11 4 CT; computed tomography
- 12
- 13
- 14
- 15 5 CO₂; carbon dioxide
- 16
- 17
- 18 6 MHR; major hepatic resection
- 19
- 20
- 21
- 22 7 BDR; extrahepatic bile duct resection
- 23
- 24
- 25 8 PD; pancreaticoduodenectomy
- 26
- 27
- 28
- 29 9 IDUS; intraductal ultrasonography
- 30
- 31
- 32
- 33 10 POCS; peroral cholangioscopy
- 34
- 35
- 36 11 CIS; carcinoma in situ
- 37
- 38
- 39
- 40 12 IC; invasive cancer
- 41
- 42
- 43 13 NM; negative margin
- 44
- 45
- 46
- 47 14
- 48
- 49
- 50
- 51
- 52
- 53
- 54
- 55
- 56
- 57
- 58
- 59
- 60
- 61
- 62
- 63
- 64
- 65

1 Introduction

2 Curative resection for biliary malignancies requires an appropriate operative plan

3 based on accurate diagnosis of tumor spread and precise understanding of the anatomy of

4 individual patients.

5 Direct cholangiography, such as endoscopic retrograde cholangiography (ERC) and

6 percutaneous transhepatic cholangiography, has been the mainstay of biliary tract imaging [1,

7 2]. However, two-dimensional (2D) cholangiography has several limitations, such as 1)

8 overlapping of the bile ducts around the hepatic hilum, 2) missing isolated branches unfilled

9 with contrast medium, 3) lack of information on the anatomical relationship in relation to the

10 vasculature, and 4) difficulty in determining the bile duct cutting line, which is restricted by

11 spatial relationship with vessels to be preserved.

12 Introduction of multi-row detector computed tomography led to progress in the

13 imaging diagnosis of cholangiocarcinoma [3]. In addition to visualizing small tumors,

14 three-dimensional (3D) demonstration of hepatic vasculature helps us to understand the

15 vascular anatomy of individual patients [4]. However, the bile duct is missed in 3D images

16 reconstructed from the conventional dynamic computed tomography (CT) protocol. Drip

17 infusion cholangiography or direct infusion of radiopaque contrast medium through a biliary

drainage tube visualizes the bile ducts as radiopaque objects and enables its 3D reconstruction [5]. However, with these methods, it is difficult to separate the bile ducts from the arteries, since the two structures are anatomically adjacent and contrasted with similar radiopacity, and they are therefore not amenable for creation of an “all-in-one” (bile ducts, arteries, and portal veins) 3D fusion image. Recently, Sugimoto et al. reported the utility of carbon dioxide (CO₂) as a radiolucent contrast material for the biliary system [6]. The radiolucent characteristics of CO₂ facilitated all-in-one 3D reconstruction by visualizing the bile ducts as radiolucent objects.

In 2009, we introduced 3DCT cholangiogram, as well as all-in-one 3D imaging, for precise understanding of the hepatic hilum anatomy, and have used it for operative planning for biliary malignancies. In the present study, our experience with 3DCT cholangiography is reviewed, with the aim of evaluating its usefulness in patients with biliary malignancies.

Methods

Study population

The study population is summarized in figure 1. We introduced 3DCT cholangiography as a routine preoperative examination on October 2009. Since that time, all

the patients with biliary malignancies who were candidates for partial liver resection with concomitant extrahepatic bile duct resection (cholangiocarcinoma and gallbladder carcinoma with hepatic hilum invasion) were prospectively enrolled. Eighty-seven patients underwent 3DCT cholangiography. Eight patients underwent a second examination after replacement or addition of biliary drainage tubes in the contralateral side because of the need for reconsideration of the operative procedures, and, as a result, 96 examinations were performed in total. Of these 87 patients, 49 underwent major hepatic resection (MHR) with extrahepatic bile duct resection (BDR) or MHR with pancreaticoduodenectomy (PD) (perihilar cholangiocarcinoma in 25 patients, extrahepatic cholangiocarcinoma extending to the perihilar region in 5 patients, intrahepatic cholangiocarcinoma with perihilar invasion in 14 patients, or gallbladder cancer with periductal invasion in 4 patients), and they were the main participants in this study. One patient had both extrahepatic cholangiocarcinoma and intrahepatic cholangiocarcinoma. Written informed consent was obtained from all patients before 3D cholangiography. The protocol for this study was approved by the institutional ethics committee. This study was registered with the University hospital Medical Information Network (unique trial number: UMIN R000018554).

3DCT cholangiography

The protocols for 3DCT cholangiography are summarized in figure 2. Of the 96 examinations, the contrast medium for the bile duct was CO₂ in 81 and iodine (30mg/ml) in 15. The choice of contrast medium was based on the severity of the bile duct stricture; CO₂ for cases with severe stricture and iodine for those with mild or no stricture. CO₂ or iodine was injected via a biliary drainage tube. The volume of injected CO₂ was 10-120 mL. It was adjusted depending on the severity of the stricture and the resistance perceived by the examiners during the injection. After confirmation of sufficient visualization of the bile ducts by a precontrast scan, a multiphase dynamic CT scan was performed in the usual manner.

In cases in which iodine was used for the bile ducts, a multiphase dynamic CT scan was performed, accompanied by an additional scan after the diluted iodine (10 – 35mL) was injected via the biliary tube.

The bile ducts, the artery, and the portal vein were extracted from the CT scan, and 3D images were constructed using image analysis programs (Virtual Place [AZE] [from October 2009 to May 2012; 62 examinations], Ziostation [Ziosoft] [from June 2012 to March 2013; 14 examinations], or Synapse Vincent [Fujifilm medicals] [from April 2013 to March 2014; 20 examinations]). In CO₂ cholangiography, the color mapping for CT colonoscopy or

lung volumetry was applied for bile duct 3D construction. The maximum order of the visualized biliary branch on 3D cholangiography was evaluated in the liver remnant, where, in most cases, the biliary drainage tube was inserted.

Hematological examination was performed on the following day in all patients to evaluate the adverse effects induced by 3D cholangiography.

Other preoperative evaluations

In all 49 patients who underwent MHR+BDR or MHR+PD, 2D cholangiography was also performed via a biliary tube. Intraductal ultrasonography (IDUS), endoscopic ultrasonography, and peroral cholangioscopy (POCS) were performed in 30, 17, and 9 cases, respectively. Tumor biopsy under ERC or POCS was performed in 36 patients. Step biopsy to determine the cutting line of the bile duct was done in 36 patients.

Operative planning and procedures using 3D imaging

Longitudinal spread was evaluated based on the combination of 2D/3D cholangiography, axial and coronal CT scan images, IDUS, POCS, and step biopsy. Tumor extension was mapped onto the 3D bile duct image. The 3D bile duct image was merged with

3D images of the artery and the portal vein to generate an “all-in-one” 3D image of the hepatic hilum. The anatomical relationships between tumor spread and the landmarks that restrict the cutting line of the bile ducts in each operative procedure were evaluated. The landmark was the umbilical portion for right side hepatectomy (U point) and the anterior branch of the right portal vein for left side hepatectomy (A point) (Figure 3, please see Video 1 as well). The peripheral limit of the bile duct cutting line was the left border of the U point in right trisectionectomy (Figure 3 I), the right border of the U point in right hemihepatectomy (Figure 3 II), the left border of the A point in left hemihepatectomy (Figure 3 III), and the right border of the A point in left trisectionectomy (Figure 3 IV). When tumor spread went beyond the left border of the U point or the right border of the A point, curative resection was judged impossible. When tumor spread was within the aforementioned limit, the possible operative procedures were listed, and the most appropriate procedure was selected based on the estimated surgical margin and the functional reserve of the liver remnant with each procedure. If the liver remnant is less than 40% in patients with obstructive jaundice or less than 30%, preoperative portal vein embolization was performed to promote hypertrophy of the remnant. The expected number of bile duct orifices on the stump of the bile duct was counted based on 3D cholangiography and compared with the actual number

that appeared on the stump during surgery to evaluate the agreement of the predicted and the actual cutting line of the bile duct.

The necessity for reconstruction of the artery or the portal vein was first assessed by 3D imaging. If the vessels that needed to be preserved were close to the tumor, tumor involvement was evaluated on the 2DCT images. Absence of fat density around the vessel was regarded as a sign of vascular invasion, and reconstruction was planned using the 3D image. Figure 4 shows a case of intrahepatic cholangiocarcinoma in the left lobe that necessitated both arterial and portal vein reconstruction. The 3D image shows the right hepatic artery and the bifurcation of the portal vein were involved by the tumor (Figure 4a). The planning of vascular reconstruction was done with the 3D image, and it was properly carried out (Figure 4b, please see Video 2 as well).

Histological evaluation

Histological involvement of cancer cells on the proximal bile duct stump was evaluated by intra-operative frozen section examination in all cases. When carcinoma in situ (CIS) or invasive cancer (IC) was observed, additional resection of the bile duct with or without parenchymal resection was considered. Histological involvement of the proximal bile duct

1 stump, dissection plane, and vasculatures were evaluated and confirmed by permanent

2
3
4 2 histopathological examination.
5
6
7

8 3
9

10
11 4 Statistical analysis
12
13
14

15 5 All statistical analyses were performed using SAS software (JMP 11.0.1; SAS

16
17
18 6 Institute Inc). Continuous variables were expressed as mean values±standard division or

19 7 medians with ranges, and compared using Student T-tests. Categorical variables were

20
21
22 8 compared using chi-square tests. A *P*-value less than 0.05 was considered statistically

23
24
25
26 9 significant.
27
28
29
30
31

32 10
33
34
35
36 11 Results
37
38
39

40 12 Patients' and tumor characteristics
41
42

43 13 Characteristics of the patients who underwent 3DCT cholangiography were

44
45
46 14 summarized in table 1. There was no significant difference between two contrast mediums.
47
48
49

50 15
51
52
53 16 Image quality
54
55
56
57
58
59
60
61
62
63
64
65

In 96 examinations, the maximum order of the visualized biliary branch on 3D

cholangiography was the second-order in 1, the third-order in 8, the fourth-order in 17, the

fifth-order in 48, and the sixth-order in 22 examinations. The median was the fifth-order, and

there was no significant difference between CO₂ and radiopaque contrast media examinations.

Adverse effects

All patients tolerated CT cholangiography without serious complications. Three

patients had mild elevations of liver enzymes. One patient undergoing CO₂ cholangiography

developed cholangitis requiring antibiotic therapy.

Type of surgery

Overall, 37 patients and 12 patients underwent MHR+BDR and MHR+PD,

respectively. The type of liver resection was right hemihepatectomy in 22 patients (45%), left

hemihepatectomy in 13 patients (27%), right trisectionectomy in 4 patients (8%), and left

trisectionectomy in 10 patients (20%). The median operative time was 702 minutes (range:

456 to 1725), with median blood loss of 1420 g (range: 310 to 21736). There were no

operative deaths.

Vascular reconstruction

In 49 patients who underwent MHR+BDR or MHR+PD, portal vein reconstruction

was potentially required on preoperative evaluation in 18 patients. All of these 18 patients

underwent portal vein reconstruction, and 14 (78%) had histologically proven portal vein

involvement. One patient required unexpected portal vein reconstruction because of severe

adhesions induced by periductal inflammation. As for the necessity for portal vein

reconstruction, the sensitivity, specificity, and accuracy of preoperative examination were

95%, 100%, and 98%, respectively.

With respect to arterial invasion, 6 patients were preoperatively diagnosed as having

arterial invasion. Of these 6 patients, 5 (83%) actually required arterial reconstruction, and 3

(50%) had histologically proven arterial involvement. Two patients required arterial

reconstruction contrary to preoperative examinations. However, histopathological

examinations revealed no arterial involvement in these patients. As a result, the sensitivity,

specificity and accuracy of preoperative examinations for arterial reconstruction were 71%,

98%, and 94%, respectively.

Bile duct orifices

In the 49 patients, the expected number of bile duct orifices was 1 to 4 (median, 2), which was in agreement with the actual number in all patients (n=49, 100%).

Surgical radicality

Histological involvement of cancer cells on the proximal bile duct stump was evaluated in the 49 patients. A negative margin (NM) was obtained in 39 patients (80%), whereas CIS and IC were observed in 7 patients (14%) and 3 patients (6%), respectively, on the first cutting. Additional resection of the bile duct was performed in 8 patients (5 patients with CIS and 3 patients with IC), and NM was obtained in 3 patients (2 patients with CIS and 1 patient with IC). In 2 patients, additional resection was abandoned. Eventually, histological evaluation of the bile duct stump was NM in 42 patients (86%), CIS in 5 patients (10%), and IC in 2 patients (4%). Results of histological examination on the proximal bile duct stump were summarized in figure 5. R0 resection was obtained in all 42 patients with NM on the bile duct stump. R0 and R1 resection rate was 86% and 14%, respectively.

Comparison of operative curability with historical controls

To explore the impact of preoperative 3D evaluation on operative planning and outcomes, our cases who underwent MHR+BDR or MHR+PD before the introduction of 3D cholangiography (from January 2004 to August 2009: n=69) were reviewed, and patients' characteristics, tumor factors, and operative outcomes were compared between the present series and the historical cohort (Table 2). In the historical control group, the type of liver resection was right hemihepatectomy in 23 patients (33%), left hemihepatectomy in 22 patients (32%), right trisectionectomy in 14 patients (20%), and left trisectionectomy in 10 patients (14%). A non-significant downward trend in right trisectionectomy was evident after the introduction of 3D cholangiography (20% vs. 8%).

MHR+PD, portal vein reconstruction, and arterial reconstruction were performed in 7 patients (10%) each. A significant difference was observed in the ratio of patients undergoing portal vein reconstruction ($p=0.0002$).

Histopathological evaluation of the bile duct stump on the first cutting was NM in 51 patients (74%), CIS in 4 patients (6%), and IC in 14 patients (20%). Additional resection was performed in 15 patients (3 patients with CIS and 12 patients with IC), and NM was obtained in 12 patients. One patient with IC on the first cutting had CIS after the additional resection. Eventually, histological evaluation of the bile duct stump was NM in 61 patients

(88%), CIS in 3 patients (4%), and IC in 5 patients (7%). The invasive cancer-free rate on the first cutting was significantly better in the present series ($p=0.02$), although the difference diminished after additional resections. In the historical control patients who obtained NM of the bile duct stump, thirteen patients resulted in R1 resection because of positive margin of the dissection plane in 9 patients, IC and CIS of bile duct stump by permanent pathological examination in 1 patient, positive margin of portal vein cut end in one patient and distant lymph node metastasis in 1 patient. As a result, R0 resection was achieved in 48 patients (70%). Although not statistically different, there was upward trend in the rate of R0 resection in the present series (70% vs. 86%).

Anatomical variations identified by all-in-one 3D images

Significant anatomical variations for biliary surgery were identified by all-in-one 3D images. Figure 6a shows an infraportal bile duct branch of the Spiegel lobe, which hampers en bloc resection during right hemihepatectomy with caudate lobectomy unless the portal vein is transected and anastomosed (please see Video 3a as well). Figure 6b shows an infraportal bile duct branch of segment 3 (please see Video 3b as well). Figure 6c shows an anatomical variation of the right posterior branch of the artery, in which A6 runs infraportally,

whereas A7 runs supraportally (please see Video 3c as well). This variation is potentially dangerous during left trisectionectomy, since, without recognizing this variation, A7 may be mistaken for the right anterior branch and be transected. Figure 6d shows an extremely rare but significant anatomical variation for right trisectionectomy. A2, A3, and A4 arose independently, and A2 ran medially and cranially to the left portal vein and was involved by the tumor (please see Video 3d as well). Without knowing this variation, A2 may be mistaken for A4, and the artery may be transected proximal to the bifurcation of A2.

Discussion

For biliary tract malignancies, curative resection is essential for improving long-term survival, but the curative resection rate remains unsatisfactory in many reports [1, 7-13]. Obstacles to curative resection are not only difficulty in making an accurate diagnosis of tumor spread, but also difficulty in the choice of an appropriate operative procedure due to the complicated anatomy of the hepatic hilum. We introduced 3DCT cholangiography to facilitate the proper choice of operative procedure based on a precise understanding of the hilar anatomy of individual patients. In this study, our series was reviewed, and its impact on outcomes was evaluated.

The multidirectional view of 3D cholangiography tells us the appropriate angle on which the diagnostically important portion of the bile duct is evaluable without overlapping, which in turn helps us perform complete 2D cholangiography using 3D cholangiography as a reference image. In addition, IDUS, POCS, and histological assessment of bile duct biopsy specimens are now practical for precise diagnosis of longitudinal tumor spread [1, 2]. Projection of the examinations onto 3D cholangiography creates a 3D map of tumor spread, which maximizes the usefulness of these fine examinations.

MRCP can noninvasively reconstruct 3D imaging of the biliary tract, which is likely to be considered a competing imaging modality to 3DCT cholangiography [14, 15]. An advantage of 3DCT cholangiography over MRCP is that it can provide all-in-one 3D fusion images of all important structures in the hepatic hilum [16]. The fusion image makes it possible to evaluate tumor spread in relation to anatomical landmarks such as the U point and A point. This is particularly important for planning operative procedures, since the bile duct cutting line is restricted by these landmarks. Agreement of the number of the orifices appearing on the bile duct stump suggests that 3D fusion images correctly predict the actual cutting line of the bile duct. The improvement in the rate of negative ductal margin on first

cutting after the introduction of 3DCT cholangiography may be partly attributable to selection of the appropriate operative procedure.

Another benefit of 3D fusion images is recognition of anatomical variations.

Variations described in figure 6 are easily missed with 2D images or separated 3D images, but they are readily recognized with all-in-one 3D fusion images. Preoperative recognition of these variations is vital for performing operations smoothly and avoiding serious complications.

Vascular invasion is frequent in biliary malignancies and is another important factor affecting operative procedures [17]. With all-in-one fusion images, surgeons can easily recognize vessels to be preserved in the planned operations and the distance between the vessels and the tumor. The 3D images objectively demonstrate suspicious portions of vascular invasion and prepare us to be ready for reconstruction during the operation. Indeed, the necessity for vascular reconstruction was predictable in all but two cases in the present series. In addition, the all-in-one 3D images provide planning of vascular reconstruction that is easily understandable even for less experienced surgeons.

Endo has already reported the usefulness of 3DCT cholangiography [9]. The uniqueness of the present study was that CO₂ was used preferentially as the contrast material.

The reason for preferential use of CO₂ is that CO₂ behaves as a negative contrast medium. A negatively-enhanced bile duct can be easily separated from positively-enhanced vessels, which enables 3D reconstruction of both the hepatic artery and the bile duct on the basis of the arterial phase and, thereby, avoids slice gaps between multiple phases caused by inconsistent breath-holding. Another advantage of CO₂ over a radiopaque agent may be the low incidence of cholangitis. Only one patient in the present series and no patients in the previous study by Sugimoto et al. suffered from cholangitis [6]. These incidences of cholangitis were relatively lower than that of previous reports in which radiopaque agent were used as contrast medium [18, 19]. The reason for the low incidence of cholangitis may be because CO₂ leaks even through severe strictures, which prevents excessive elevation of intraductal pressure during injection.

However, 3DCT cholangiography has several limitations. First, 3DCT cholangiography is not an alternative to other diagnostic examinations such as IDUS, POCS, and 2D cholangiography. The resolution of 3D images is restricted by, and therefore cannot be superior to, that of the original CT images. Sensitivity of 3D cholangiography for subtle changes or irregularities on the bile duct mucosa should not be as high as that of 2D cholangiography. We would like to emphasize that 3DCT cholangiography is useful not for

1 fine diagnosis of tumor extension but as a reference image for the other diagnostic modalities
2
3
4 2 and appropriate operative planning based on precise understanding of biliary anatomy. Second,
5
6
7
8 3 the quality of images is somewhat dependent on experience, because CT cholangiography is
9
10
11 4 not a real-time fluoroscopic examination. The choice and the volume of contrast material
12
13
14
15 5 (either CO₂ or radiopaque agent) to be injected should be adjusted according to the severity of
16
17
18
19 6 the stricture.
20
21

22 7 In conclusion, 3D cholangiography and all-in-one 3D fusion images of the hepatic
23
24
25 8 hilum provide accurate information about hilar anatomy and play a role in adequate operative
26
27
28
29 9 planning. They also facilitate precise implementation of the planned surgery. We hope this
30
31
32
33 10 technique will become widespread and improve the prognosis of patients with biliary
34
35
36 11 malignancies by refining the complicated operations required for these intractable diseases.
37
38
39

40 12

41
42 13
43
44
45
46
47
48
49
50
51
52
53
54
55
56
57
58
59
60
61
62
63
64
65

References

1. Endo I, Matsuyama R, Mori R, Taniguchi K, Kumamoto T, Takeda K, et al. Imaging and surgical planning for perihilar cholangiocarcinoma. *J Hepatobiliary Pancreat Sci.* 2014 Feb 12.
2. Ito F, Agni R, Rettammel RJ, Been MJ, Cho CS, Mahvi DM, et al. Resection of hilar cholangiocarcinoma: Concomitant liver resection decreases hepatic recurrence. *Ann Surg.* 2008 Aug;248(2):273-9.
3. Kim HJ, Lee DH, Lim JW, Ko YT. Multidetector computed tomography in the preoperative workup of hilar cholangiocarcinoma. *Acta Radiol.* 2009 Oct;50(8):845-53.
4. Lu BC, Ren PT. Treatment of hilar cholangiocarcinoma of bismuth-corlette type III with hepaticojejunostomy. *Contemp Oncol (Pozn).* 2013;17(3):298-301.
5. Luo X, Yuan L, Wang Y, Ge R, Sun Y, Wei G. Survival outcomes and prognostic factors of surgical therapy for all potentially resectable intrahepatic cholangiocarcinoma: A large single-center cohort study. *J Gastrointest Surg.* 2014 Mar;18(3):562-72.
6. Sugimoto M, Yasuda H, Koda K, Suzuki M, Yamazaki M, Tezuka T, et al. Carbon dioxide-enhanced virtual MDCT cholangiopancreatography. *J Hepatobiliary Pancreat Sci.* 2010 Sep;17(5):601-10.

- 1 7. Machado MA, Makdissi FF, Surjan RC. Right trisectionectomy with principle en bloc
- 2
- 3
- 4 2 portal vein resection for right-sided hilar cholangiocarcinoma: No-touch technique. Ann Surg
- 5
- 6
- 7
- 8 3 Oncol. 2012 Apr;19(4):1324-5.
- 9
- 10
- 11 4 8. Chen W, Ke K, Chen YL. Combined portal vein resection in the treatment of hilar
- 12
- 13
- 14
- 15 5 cholangiocarcinoma: A systematic review and meta-analysis. Eur J Surg Oncol. 2014
- 16
- 17
- 18 6 May;40(5):489-95.
- 19
- 20
- 21
- 22 7 9. Endo I, Shimada H, Sugita M, Fujii Y, Morioka D, Takeda K, et al. Role of
- 23
- 24
- 25 8 three-dimensional imaging in operative planning for hilar cholangiocarcinoma. Surgery. 2007
- 26
- 27
- 28 9 Nov;142(5):666-75.
- 29
- 30
- 31
- 32
- 33 10 10. Hirano S, Kondo S, Tanaka E, Shichinohe T, Tsuchikawa T, Kato K, et al. Outcome of
- 34
- 35
- 36 11 surgical treatment of hilar cholangiocarcinoma: A special reference to postoperative morbidity
- 37
- 38
- 39 12 and mortality. J Hepatobiliary Pancreat Sci. 2010 Jul;17(4):455-62.
- 40
- 41
- 42
- 43 13 11. Igami T, Nishio H, Ebata T, Yokoyama Y, Sugawara G, Nimura Y, et al. Surgical treatment
- 44
- 45
- 46 14 of hilar cholangiocarcinoma in the "new era": The nagoya university experience. J
- 47
- 48
- 49 15 Hepatobiliary Pancreat Sci. 2010 Jul;17(4):449-54.
- 50
- 51
- 52
- 53
- 54
- 55
- 56
- 57
- 58
- 59
- 60
- 61
- 62
- 63
- 64
- 65

12. Matsumoto N, Ebata T, Yokoyama Y, Igami T, Sugawara G, Shimoyama Y, et al. Role of anatomical right hepatic trisectionectomy for perihilar cholangiocarcinoma. *Br J Surg*. 2014 Feb;101(3):261-8.
13. Mavros MN, Economopoulos KP, Alexiou VG, Pawlik TM. Treatment and prognosis for patients with intrahepatic cholangiocarcinoma: Systematic review and meta-analysis. *JAMA Surg*. 2014 Apr 9.
14. Miyazaki M, Kimura F, Shimizu H, Yoshidome H, Otuka M, Kato A, et al. One hundred seven consecutive surgical resections for hilar cholangiocarcinoma of bismuth types II, III, IV between 2001 and 2008. *J Hepatobiliary Pancreat Sci*. 2010 Jul;17(4):470-5.
15. Nguyen K, Sing JT, Jr. Review of endoscopic techniques in the diagnosis and management of cholangiocarcinoma. *World J Gastroenterol*. 2008 May 21;14(19):2995-9.
16. Kalra VB, Gilbert JW, Krishnamoorthy S, Cornfeld D. Value of non-contrast sequences in magnetic resonance angiography of hepatic arterial vasculature. *Eur J Radiol*. 2014 Jun;83(6):905-8.
17. Rocha FG, Matsuo K, Blumgart LH, Jarnagin WR. Hilar cholangiocarcinoma: The memorial sloan-kettering cancer center experience. *J Hepatobiliary Pancreat Sci*. 2010 Jul;17(4):490-6.

- 1 18. Bai Y, Gao F, Gao J, Zou DW, Li ZS. Prophylactic antibiotics cannot prevent endoscopic
- 2
- 3
- 4 2 retrograde cholangiopancreatography-induced cholangitis: A meta-analysis. *Pancreas*. 2009
- 5
- 6
- 7
- 8 3 *Mar*;38(2):126-30.
- 9
- 10
- 11 4 19. Zhang R, Zhao L, Liu Z, Wang B, Hui N, Wang X, et al. Effect of CO2 cholangiography
- 12
- 13
- 14
- 15 5 on post-ERCP cholangitis in patients with unresectable malignant hilar obstruction - a
- 16
- 17
- 18 6 prospective, randomized controlled study. *Scand J Gastroenterol*. 2013 Jun;48(6):758-63.
- 19
- 20
- 21
- 22
- 23
- 24
- 25
- 26
- 27
- 28
- 29
- 30
- 31
- 32
- 33
- 34
- 35
- 36
- 37
- 38
- 39
- 40
- 41
- 42
- 43
- 44
- 45
- 46
- 47
- 48
- 49
- 50
- 51
- 52
- 53
- 54
- 55
- 56
- 57
- 58
- 59
- 60
- 61
- 62
- 63
- 64
- 65

1 Figure legends

2 Figure 1

3 Summary of the study population in the present study

4 Eighty seven patients with biliary tract malignancy underwent three-dimensional computed
5 tomography (3DCT) cholangiography between October 2009 and September 2014. Of these
6 patients, 21 patients did not undergo laparotomy for the following reasons: 3 patients had
7 distant metastases (liver metastases in 2 patients and supraclavicular lymph node metastases
8 in 1 patient); 10 patients had excessive tumor spread (longitudinal in 6 patients and vertical in
9 4 patients); 5 patients had insufficient remnant liver volume; 2 patients refused surgical
10 treatment; and 1 patient died of primary disease prior to surgery. Sixty-six patients underwent
11 laparotomy. Resection was abandoned after laparotomy in 10 patients, because of distant
12 metastases in 7 patients (peritoneal dissemination in 4 patients, para-aortic lymph node
13 metastases in 2 patients and liver metastases in 1 patient) and vertical tumor invasion to the
14 duodenum in 3 patients. Fifty-six patients underwent resection with curative intent. Of these
15 56 patients, 3 underwent hepatectomy without extrahepatic bile duct resection, and 4
16 underwent pancreaticoduodenectomy (PD) without liver resection. Eventually, forty-nine
17 patients underwent major hepatic resection (MHR) with extrahepatic bile duct resection

(BDR) or MHR with pancreaticoduodenectomy (MHR + PD). Sixty nine patients who

underwent MHR + BDR or MHR + PD before the introduction of 3DCT cholangiography

were served as the historical control.

CCA; Cholangiocarcinoma

Figure 2

The protocol for 3-dimensional computed tomography cholangiography with carbon dioxide

as the contrast medium for the bile duct (a) and with iodine as contrast medium for the bile

duct (b).

All imaging was performed using a 64-multi-row detector computed tomography scanner

(Aquilion 64, Toshiba Medical Systems, Tochigi, Japan). Scanning parameters were 120 kVp,

approximately 250-350 mAs adjusted according to patient size (minimum 140 to maximum

500 mAs [Sure Exposure, Toshiba Medical Systems]), 0.5-mm section collimation, and a

pitch factor of 0.828 during a single breath-hold volumetric acquisition. Images were obtained

in a craniocaudal direction and reconstructed with 1-mm slice thickness and 1-mm intervals.

Nonionic iodinated contrast material (Iomeron 350; Esai Co, Ltd, Tokyo, Japan) at 2 mL/kg

with a maximum dose of 135 mL was injected through the antecubital vein at a rate of 4 mL/s.

Using a bolus tracking system (Sure Start, Toshiba Medical Systems) with a trigger of the aorta reaching 120 HU, a four-phase scan was obtained, with unenhanced, first phase (5 seconds after the trigger), second phase (20 seconds after the trigger), and third phase (50 seconds after the trigger) images.

Figure 3

Estimation of the bile duct cutting line by 3D fusion image of the bile duct and the portal vein

The cutting line of the bile duct is restricted by the landmarks on the portal vein. The cutting line of the bile duct in right trisectionectomy (I) and right hemihepatectomy (II) is around the left border and the right border of the umbilical portion (U) of the portal vein, respectively, whereas that in left hemihepatectomy (III) and left trisectionectomy (IV) is around the left border and the right border of the anterior branch (A) of the portal vein, respectively.

Figure 4

Planning of vascular reconstruction by all-in-one 3D fusion images

1 The all-in-one fusion image (a) shows that both the right portal vein and right hepatic artery
2
3
4
5 2 are involved by tumor, but sufficient lengths were preserved for anastomosis. Planning of
6
7
8 3 vascular reconstruction was made on the 3D image, and it was implemented (b).
9
10
11 4 (Red arrow; Right hepatic artery, White arrow; Right portal vein, Yellow arrow; Bile duct
12
13
14
15 5 cutting line, Asterisk; Tumor, Black line; Cutting line of the hepatic artery, Black dotted line;
16
17
18 6 Cutting line of the portal vein)
19
20
21
22 7
23
24
25 8 Figure 5
26
27
28
29 9 Histological evaluation on the proximal bile duct stump
30
31
32
33 10 NM was obtained in 39 patients (80%) on the first cutting. Additional resection of the bile
34
35
36 11 duct was performed in 8 patients (5 patients with CIS and 3 patients with IC), and NM was
37
38
39
40 12 obtained in 3 patients (2 patients with CIS and 1 patient with IC). In 2 patients with CIS,
41
42
43 13 additional resection was abandoned. Eventually, histological evaluation of the bile duct stump
44
45
46
47 14 was NM in 42 patients (86%), CIS in 5 patients (10%), and IC in 2 patients (4%).
48
49
50
51 15 MHR; Major hepatic resection, BDR; Extrahepatic bile duct resection, PD;
52
53
54 16 Pancreaticoduodenectomy, NM; Negative margin, CIS; Carcinoma in situ, IC; Invasive
55
56
57 17 cancer
58
59
60
61
62
63
64
65

- 1
 - 2
 - 3
 - 4
 - 5
 - 6
 - 7
 - 8
 - 9
 - 10
 - 11
 - 12
 - 13
 - 14
 - 15
 - 16
 - 17
 - 18
 - 19
 - 20
 - 21
 - 22
 - 23
 - 24
 - 25
 - 26
 - 27
 - 28
 - 29
 - 30
 - 31
 - 32
 - 33
 - 34
 - 35
 - 36
 - 37
 - 38
 - 39
 - 40
 - 41
 - 42
 - 43
 - 44
 - 45
 - 46
 - 47
 - 48
 - 49
 - 50
 - 51
 - 52
 - 53
 - 54
 - 55
 - 56
 - 57
 - 58
 - 59
 - 60
 - 61
 - 62
 - 63
 - 64
 - 65
- 1
- 2 Figure 6
- 3 All-in-one 3D images of significant anatomical variations
- 4 a) Infraportal bile duct branch of the Spiegel lobe. The bile duct branch of the Spiegel
- 5 lobe (blue) runs caudally to the left portal vein (white arrow).
- 6 b) Infraportal bile duct branch of segment 3. The bile duct branch of Couinaud's
- 7 segment 3 (blue) runs caudally to the portal vein (white arrow).
- 8 c) An anatomical variation of the right posterior branch of the artery. A6 (orange) runs
- 9 infraportally, and A7 (blue) runs supraportally.
- 10 d) An anatomical variation of the left hepatic artery. A2 (blue), A3, and A4 arise
- 11 independently, and A2 runs medially and cranially to the left portal vein and is
- 12 involved by the tumor.
- 13

Table 1 Patients' characteristics; 3DCT cholangiography

Contrast media	CO2 (n=81)	Iodine (n=15)	<i>P</i> value
age	64±10	64±15	n.s.
gender (male/female)	55/26	11/4	n.s.
Location of tumor			
Perihilar	43% (n=34)	47% (n=7)	
Extrahepatic	17% (n=14)	0% (n=0)	
Intrahepatic	27% (n=22)	47% (n=7)	
Gallbladder	12% (n=10)	7% (n=1)	
Intrahepatic and extrahepatic	2% (n=1)		
Biliary drainage			
ENBD	86% (n=70)	100% (n=15)	
PTBD	7% (n=5)	0% (n=0)	
Both	6% (n=6)	0% (n=0)	
Maximum order of the visualized biliary branch	5 (3-6)	5 (3-6)	n.s.
Adverse effect			
Cholangitis	1% (n=1)	0% (n=0)	
Elevation of liver enzyme	1% (n=1)	13% (n=2)	
Post 3DCT hematological biomarkers			
WBC (10 ³ /μL)	5.5±3.3	6.1±1.9	n.s.
AST (IU/L)	60±46	42±19	n.s.
ALT (IU/L)	99±87	53±25	n.s.
T.Bil (mg/dL)	2.0±2.9	1.3±0.9	n.s.
LDH (IU/L)	190±72	170±28	n.s.
ALP (IU/L)	699±489	802±436	n.s.
γGTP (IU/L)	321±271	371±191	n.s.

Other preoperative examinations

IDUS	63% (n=51)	47% (n=7)	n.s.
EUS	41% (n=33)	20% (n=3)	n.s.
POCS	16% (n=13)	27% (n=4)	n.s.
Tumor biopsy	72% (n=58)	67% (n=10)	n.s.
Step biopsy	57% (n=46)	47% (n=7)	n.s.

ENBD; Endoscopic nasobiliary drainage,

PTBD; Percutaneous transhepatic biliary drainage,

IDUS; Intraductal ultrasonography,

EUS; Endoscopic ultrasound,

POCS; Peroral cholangioscopy

1

2

Table 2 Comparison with historical control

		3D group (n=49)	Historical group (n=69)	<i>P</i> value
age		64±11	66±9	n.s.
gender	male/female	34/15	32/37	0.01
Location of tumor	Perihilar	50% (n=25)	61% (n=42)	
	Extrahepatic	10% (n=5)	6% (n=4)	
	Intrahepatic	28% (n=14)	22% (n=15)	
	Gallbladder	8% (n=4)	12% (n=8)	
	Intrahepatic and extrahepatic	2% (n=1)		
Tumor marker	CEA	6.0±16.5	4.4±8.7	n.s.
	CA19-9	423±1476	564±1708	n.s.
Subtype of biliary cancer	Papillary type	16% (n=8)	13% (n=9)	n.s.
Type of surgery	Right hemihepatectomy	45% (n=22)	33% (n=23)	n.s.
	Left hemihepatectomy	27% (n=13)	32% (n=22)	
	Right trisectionectomy	8% (n=4)	20% (n=14)	
	Left trisectionectomy	20% (n=10)	14% (n=10)	
	MHR+PD	24% (n=12)	10% (n=7)	0.04
Vascular reconstruction	Portal vein	39% (n=19)	10% (n=7)	0.0002
	Hepatic artery	14% (n=7)	10% (n=7)	n.s.
Blood loss		2687±3685	1750±1609	n.s.
Operative time		782±277	635±123	0.0002
TNM stage	T4	43% (n=21)	17% (n=12)	0.0025
	N1	43% (n=21)	48% (n=33)	n.s.
	M	0% (n=0)	10% (n=7)	0.0052
	StageIV	41% (n=20)	35% (n=24)	n.s.

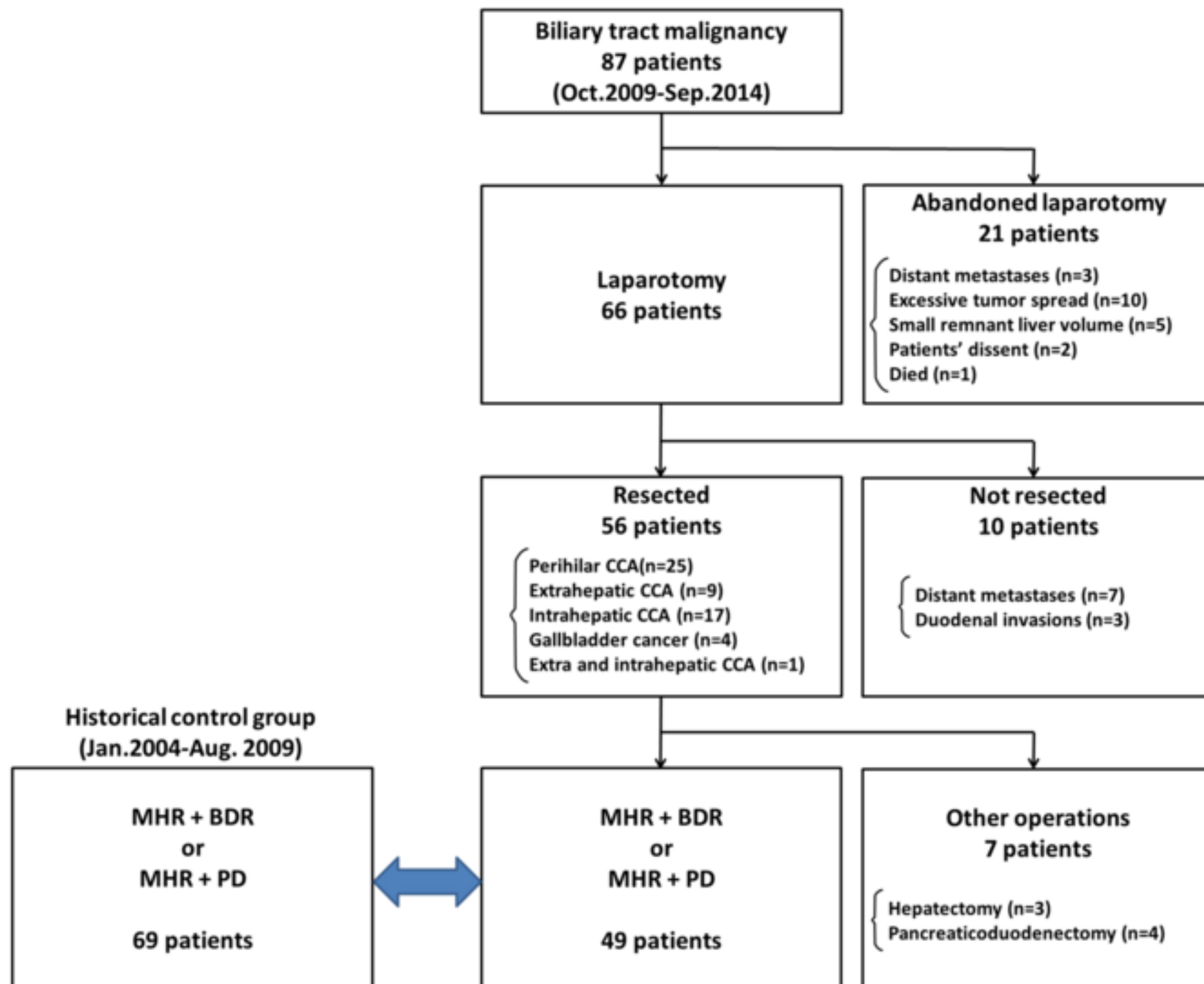
Bile duct stump				
First cutting	Negative margin	80% (n=39)	74% (n=51)	0.03
	Carcinoma in situ	14% (n=7)	6% (n=4)	
	Invasive cancer	6% (n=3)	20% (n=14)	
	Invasive cancer free ratio	94% (n=46)	80% (n=55)	0.02
Additional resection	Negative margin	86% (n=42)	88% (n=61)	n.s.
	Carcinoma in situ	10% (n=5)	4% (n=3)	
	Invasive cancer	4% (n=2)	7% (n=5)	
	Invasive cancer free ratio	96% (n=47)	92% (n=64)	n.s.
Surgical radicality	R0	86% (n=42)	70% (n=48)	n.s.

CEA; Carcinoembryonic antigen, CA19-9; Carbohydrate antigen 19-9

1
2

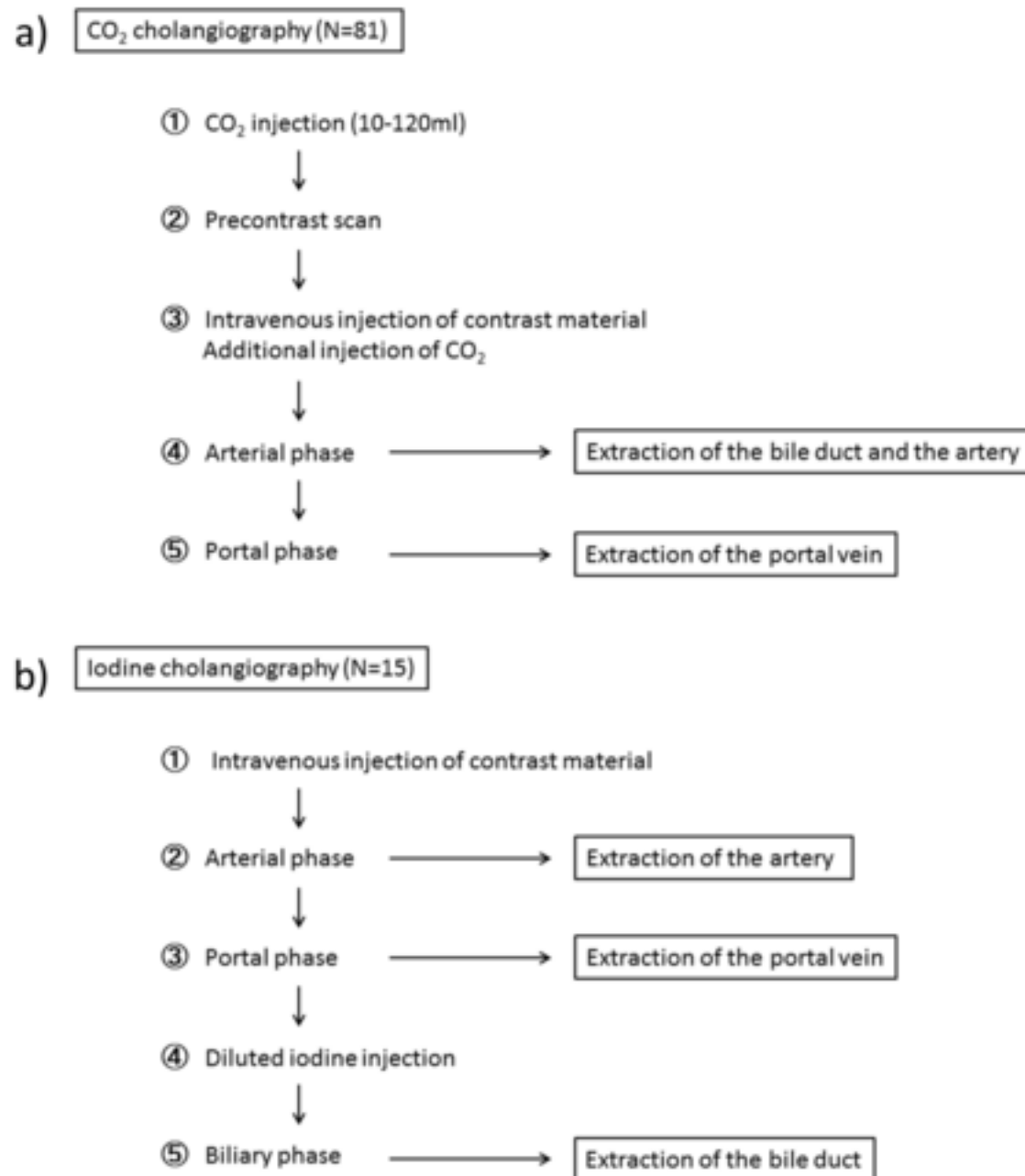
Figure

[Click here to download high resolution image](#)



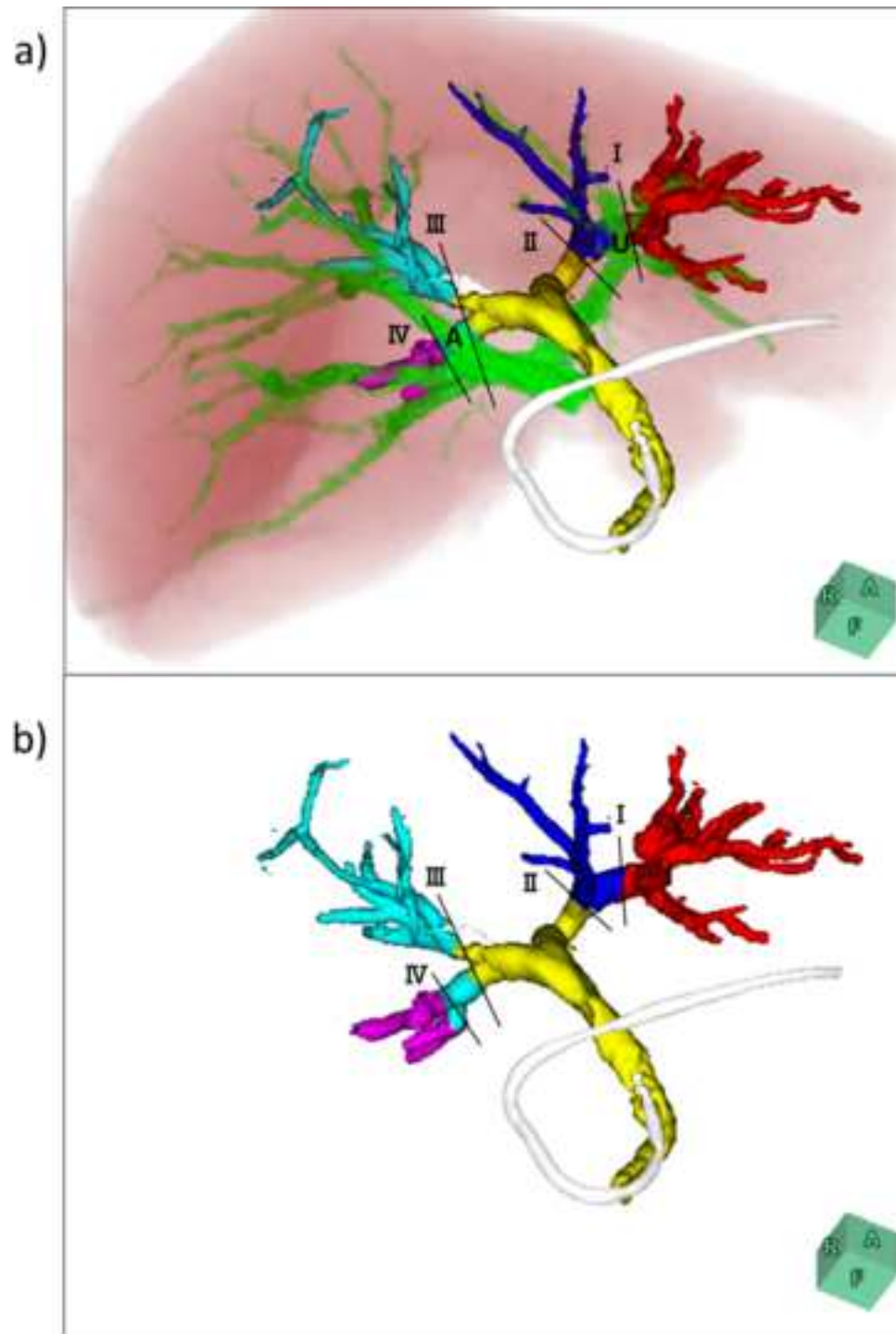
Figure

[Click here to download high resolution image](#)



Figure

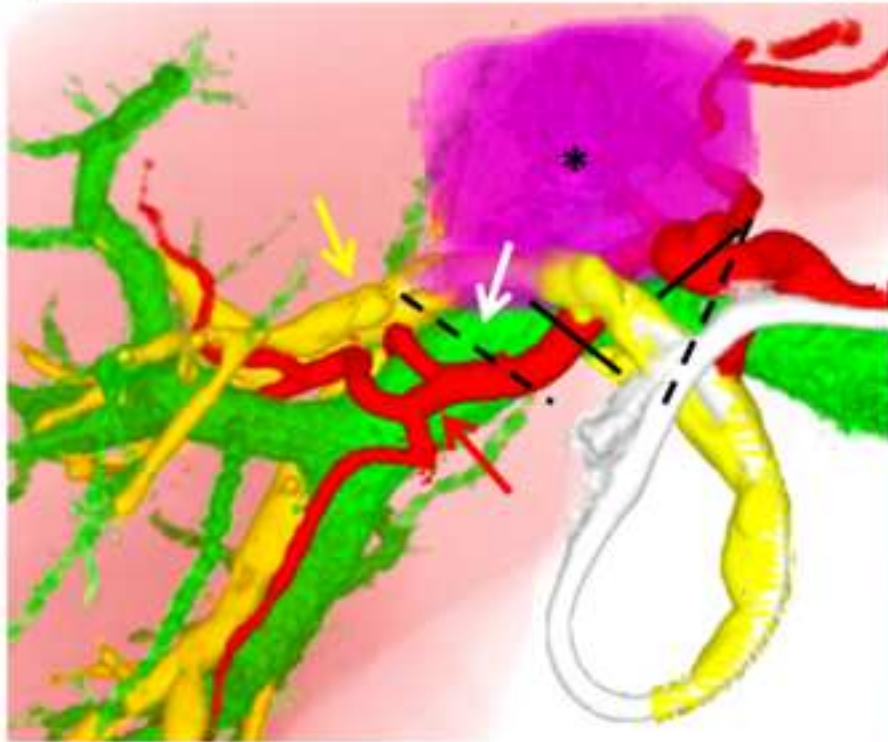
[Click here to download high resolution image](#)



Figure

[Click here to download high resolution image](#)

a)



b)

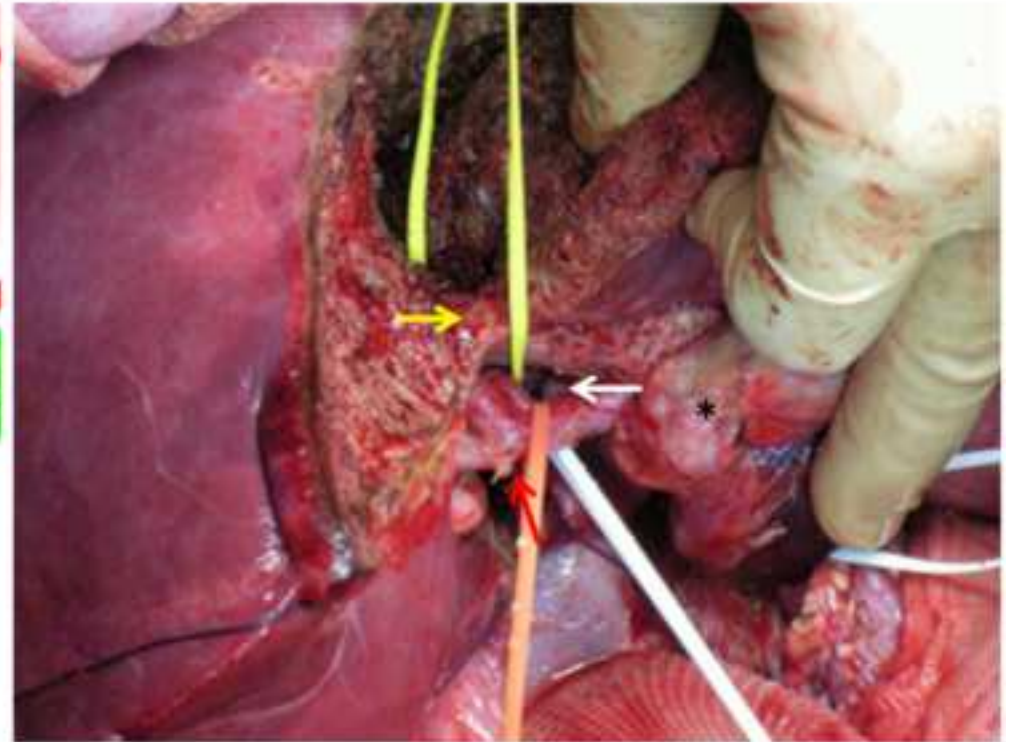
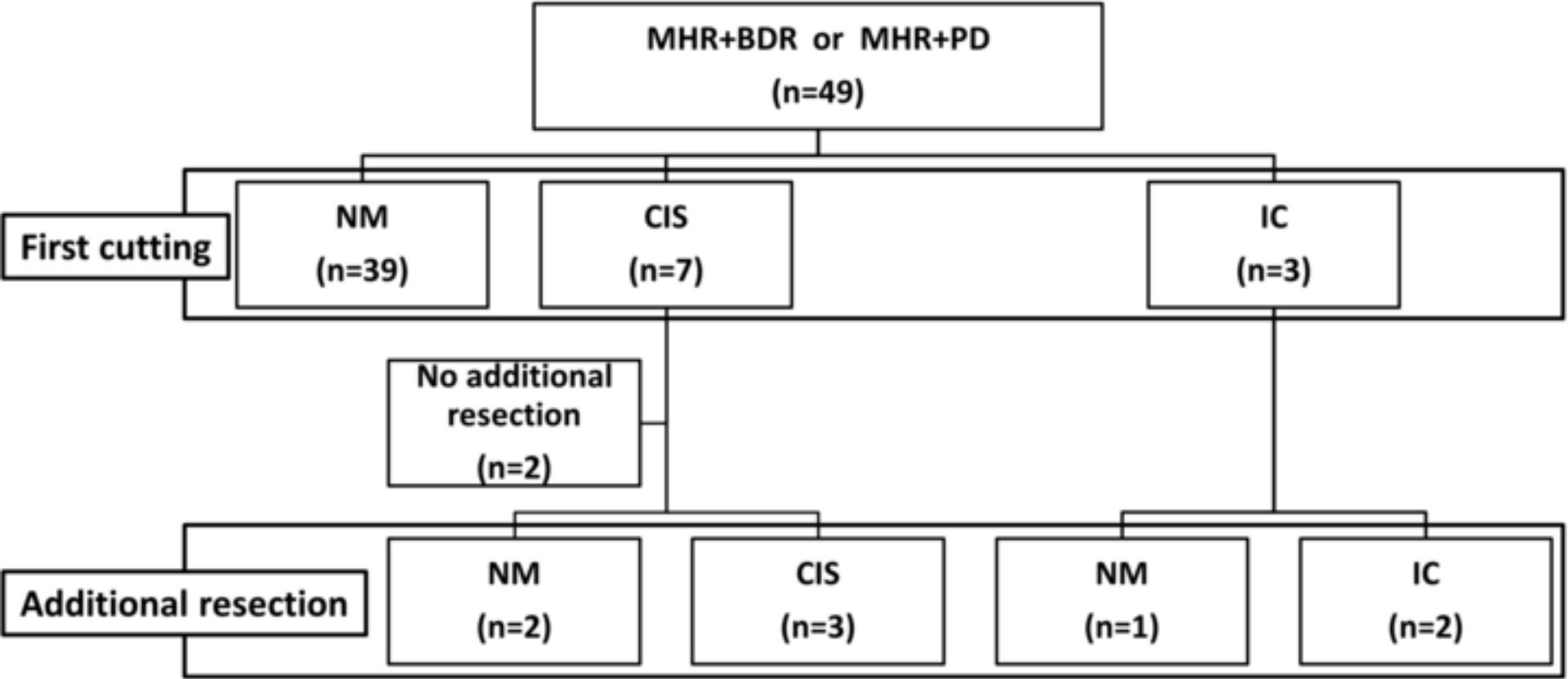
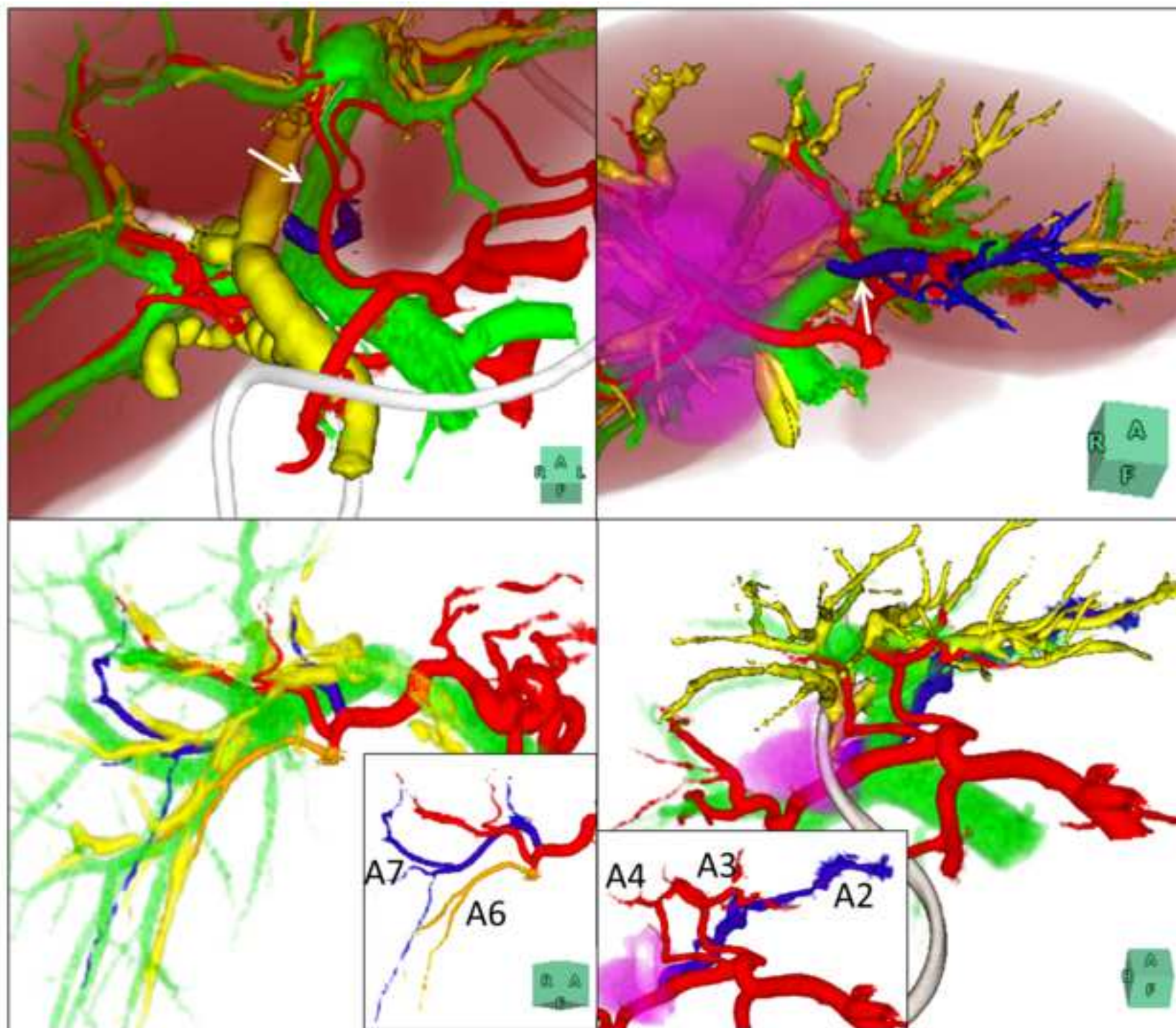


Figure
[Click here to download high resolution image](#)



Figure

[Click here to download high resolution image](#)



a	b
c	d

